NANO LETTERS

LETTER

pubs.acs.org/NanoLett

Assembling Molecular Electronic Junctions One Molecule at a Time

Andrew P. Bonifas[†,‡] and Richard L. McCreery[*,‡,§]

[†]Department of Materials Science and Engineering, The Ohio State University, 2041 College Road, Columbus, Ohio 43210, United States

[‡]National Institute for Nanotechnology, National Research Council Canada, Canada, T6G 2G2

[§]Department of Chemistry, University of Alberta, Canada,T6G 2R3

Supporting Information

ABSTRACT: Diffusion of metal atoms onto a molecular monolayer attached to a conducting surface permits electronic contact to the molecules with minimal heat transfer or structural disturbance. Surface-mediated metal deposition (SDMD) involves contact between "cold" diffusing metal atoms and molecules, due to shielding of the molecules from direct exposure to metal vapor. Measurement of the current through the molecular layer during metal diffusion permits observation of molecular conductance for junctions containing as few as one molecule. Discrete conductance steps were observed for 1−10 molecules within a monolayer during a single deposition run, corresponding to "recruitment" of additional molecules as the contact area between the diffusing Au layer and molecules increases. For alkane monolayers, the molecular conductance measured with SDMD exhibited an exponential dependence on molecular length with a decay constant (β) of 0.90 per CH_2 group, comparable to that observed by other techniques. Molecular conductance values were determined for three azobenzene molecules, and correlated with the offset between the molecular HOMO and the contact Fermi level, as expected for hole-mediated tunneling. Current−voltage curves were obtained during metal deposition showed no change in shape for junctions containing 1, 2, and 10 molecules, implying minimal intermolecular interactions as single molecule devices transitioned into several molecules devices. SDMD represents a "soft" metal deposition method capable of providing single molecule conductance values, then providing quantitative comparisons to molecular junctions containing 10^6 to 10^{10} molecules.

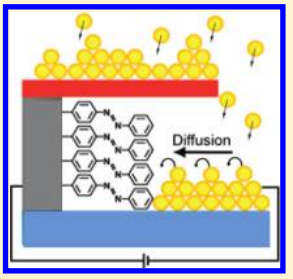

KEYWORDS: Molecular electronics, molecular junction, organic electronics, electron transport, electron tunneling

Charge transport through molecular electronic junctions has been extensively studied with the aim of correlating observed electronic behavior with molecular structure, thus allowing rational design of integrated molecular circuits. Conductance has been measured through single molecules[1,2] and molecular ensembles[3−5] (e.g., >10^3 molecules) where the electronic behavior has been reported to exhibit conductance switching[6] and orbital gating.[7] Comparison between single-molecule and many-molecule paradigms has been difficult because molecular conductance is strongly dependent on the entire molecular system, including intermolecular interactions, interfacial chemistry, and contact geometry. Here we demonstrate for the first time the ability to fabricate molecular junctions containing single to tens of molecules "one molecule at a time", allowing comparison between single molecule and molecular ensemble conductance using a single experimental paradigm. Our technique employs surface diffusion mediated deposition (SDMD) to fabricate molecular junctions without molecular damage or metal penetration, where single molecule conductance is determined through in situ current monitoring during the onset of electronic contact between the molecular layer and a metallic second contact.[8] The results demonstrate the effect of molecular length, molecular energy levels, and the number of molecules on conduction through aliphatic and aromatic molecules.

We recently introduced SDMD as a method to fabricate reproducible metallic contacts on large-area molecular layers without metal penetration or damage to the molecular layer.[8] In brief, the SDMD technique starts with depositing a metallic layer adjacent to and 30−70 nm away from a molecular layer with the molecules protected by a SiO_2 "overhang" that prevents direct metal deposition, as shown in Figure 1. Remote deposition allows the kinetic energy and heat of condensation of the depositing metal to be dissipated away from the molecular layer, thus eliminating molecular damage due to heating and metal penetration due to metal atom momentum. Surface diffusion causes the metallic layer to migrate toward and onto the molecular layer to form the second electronic contact. With surface diffusion, all adatoms contacting the molecular layer have an internal binding energy (2−3 eV) within the diffusing metal contact, thus providing a large barrier for adatom dissociation and eliminating metal penetration into the molecular layer.[9] A detailed description of device fabrication is provided in Supporting Information (Figures S1−S4).

For in situ SDMD, the junction current is monitored during the initial contact formation between the molecular layer and the

Received: July 21, 2011
Revised: September 28, 2011
Published: October 13, 2011

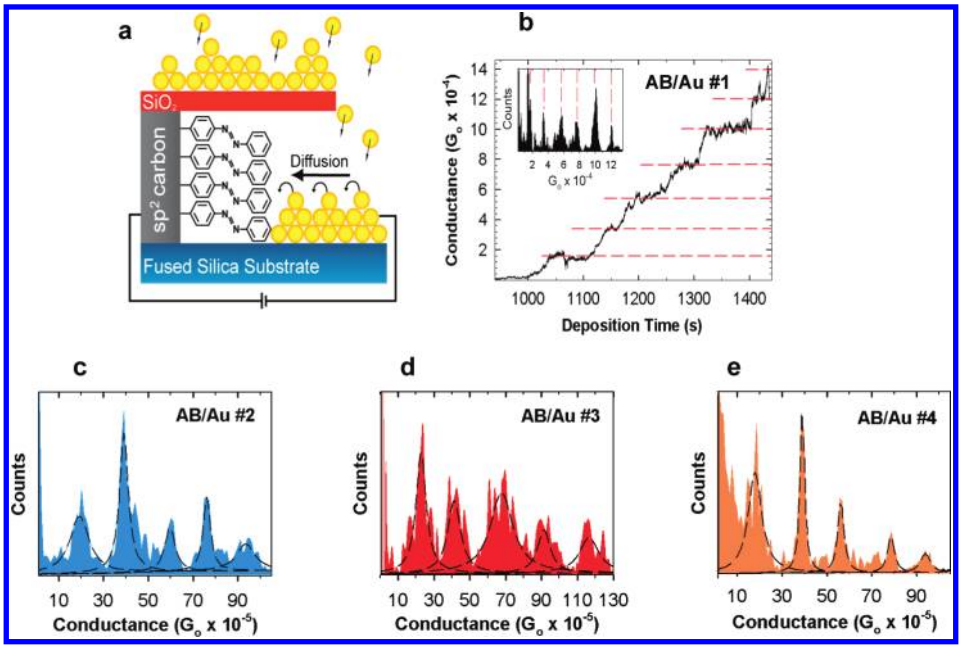

Figure 1. In-situ SDMD: (a) Schematic of the in situ SDMD technique with an azobenzene monolayer attached to the conductive sp^2 carbon sidewall. The SiO_2 "overhang" prevents the depositing Au atoms from directly landing on the sidewall, and the deposition distance away from the sidewall is controlled through the deposition angle. (b) Measured conductance vs deposition time ($V = 1.0$ V) with an azobenzene monolayer present, showing steps (conductance peaks) of 2.0×10^{-4} G_o. Horizontal dashed lines correspond to peaks in the conductance histogram. Inset shows a histogram of >24 000 data points measured every 50 ms. (c−e) Histograms for separate azobenzene devices, obtained using the same conditions as panel b. "Bin" width for histograms was ∼5% of the peak spacing, 4.8×10^{-6} G_o in this case.

diffusing metallic contact to determine the change in conductance as metal atoms contact individual molecules within a monolayer. Figure 1b shows the measured conductance versus deposition time, with the current at $V = 1$ V stated in units of G_o, the quantum of conductance ($G_o = 2e^2/h$, or 77.4 μS). Prior to the observance of nonzero current ($t < 900$ s), the thickness of the deposited Au contact was 10 nm, which ensured a continuous Au layer leading to the molecular layer. Several conductance steps are apparent in the conductance-time trace, which are more pronounced in the histogram (inset of Figure 1b) of conductance for the entire trace shown. The conductance steps are likely due to contacts forming between the diffusing Au front and individual AB molecules and have a mean spacing ($N = 22$) of $(20 \pm 3) \times 10^{-5}$ G_o, or 15.5 nS. Quantized conductance is expected when the width of the conducting channel is on the order of a Fermi wavelength[10] and has been reported previously for both molecules and amorphous carbon materials.[11] Substructure within conductance peaks is likely due to various bonding geometries at the sidewall.[12] As described in Supporting Information (Figure S5), a control experiment without a molecular layer exhibited conductance steps close to the 77.4 μS expected for a single atom contact. The observation of G_o steps in the absence of a molecular layer confirms individual contact resolution during in situ SDMD.

Single molecule conductance within a variety of monolayers was determined with the SDMD technique outlined in Figure 1 in order to determine the effect of molecular structure and length on observed conductance. As described in Supporting Information, monolayers were formed using established techniques:[13,14] diazonium reduction for azobenzene (AB), nitroazobenzene (NAB), and dimethylaminoazobenzene (DAB) and primary amine oxidation for aliphatic molecules with 4, 6, 8, and 10 carbon atoms. The SDMD geometry prevents AFM verification of the layer thickness directly, but identical deposition conditions were used on flat PPF surfaces to calibrate the layer thickness. For all seven molecules, the measured AFM thickness was (0.83 ± 0.03) times the calculated thickness for a perpendicular monolayer. This difference corresponds to an average molecular tilt angle of 34° relative to the surface normal, consistent with an independent determination using FTIR spectroscopy.[15]

For an octylamine (C_8) monolayer, conductance was measured during Au deposition (before 1300 s) and after the electron beam was turned off and deposition stopped, as shown in Figure 2a. Focusing on the increase in conductance during Au deposition, conductance steps are observed and highlighted by the dashed lines. The histogram confirms conductance steps with an average spacing of 1.4×10^{-5} G_o, as calculated by fitting Lorentzian distributions to the conductance peaks. After deposition, conductance of the formed C_8/Au junction decreased stepwise from seven contacted molecules to two molecules in about 1300 s, with a similar magnitude of the conductance steps during and after Au deposition. The conductance decrease can be attributed to Au atoms diffusing off the molecular layer toward a lower energy site within the Au lead, presumably due to the weak CH_3−Au interaction and small barrier for Au diffusion away from the molecular interface. The apparent exponential decrease in conductance is the result of the highest energy (least stable) Au atoms diffusing away first followed by lower energy atoms, and the rate of decrease was found to be dependent on the molecular end group (see Supporting Information).

Conductance histograms for a series of C_4 to C_{10} aminoalkanes during Au deposition are shown in Figure 3, in which the conductance peaks are fit with Lorentzian distributions as previously reported for single molecule junctions.[25] The histograms

dx.doi.org/10.1021/nl202495k |Nano Lett. 2011, 11, 4725–4729

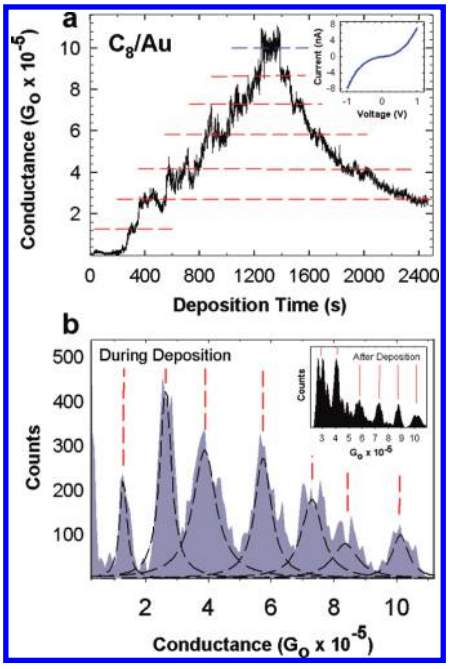

Figure 2. Molecular conductance of octylamine (C_8) monolayer: (a) Conductance versus Au deposition time for a C_8 monolayer attached to the carbon sidewall. Conductance steps of 1.4 × 10^{-5} G_o were observed during contact formation and as negative steps after Au deposition. The inset shows a current−voltage curve containing seven C_8 molecules, as determined by counting the number of previous conductance steps. (b) The conductance histogram during formation of the C_8/Au junction shows clear conductance peaks, where the center of the fitted Lorentzian distributions are projected as dashed red lines in panel a. Similar conductance peaks were observed after Au deposition, as shown in the inset to panel b. Spacing between the conductance steps and peaks is the single molecule conductance for an *n*-octylamine molecule in an *n*-octylamine monolayer. Histograms consisted of about 20 000 data points collected with an integration time of one power line cycle (16.6 ms) for each point with a "bin" width of ∼5% of the conductance peak spacing.

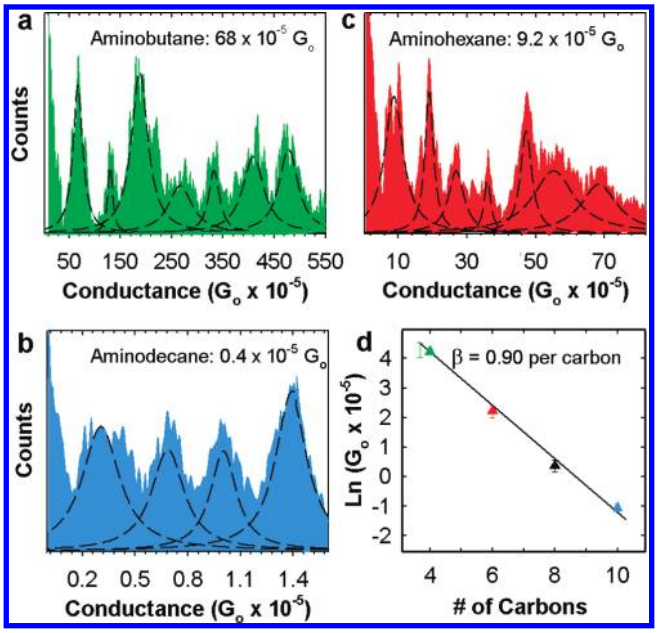

Figure 3. Molecular conductance of a series of aminoalkane molecules. (a−c) Conductance histograms for C_4, C_6, and C_{10} aminoalkane monolayers with the peaks fitted to Lorentzian distributions. The histograms were constructed from three separate junctions for C_4 and C_6, and two separate junctions for C_{10}. All histograms contained at least 12 000 data points measured every 50 ms. Spacing between the conductance peaks does not show a trend with the number of observed conductance steps. Observed substructure within individual conductance peaks are most likely caused by various molecular/Au bonding geometries. (d) The single molecule conductance decreased exponentially with molecular length with a tunneling decay constant of β = 0.90 per carbon (0.75 $Å^{-1}$).

were constructed from three separate junctions for C_4 and C_6 molecules and two separate junctions for C_{10} junctions. The conductance results are summarized in Table 1, and detailed statistics for each junction are provided in Supporting Information.

The conductance exhibits an exponential decrease with molecular length consistent with off-resonant tunneling models.[16] As shown in Figure 3d, the tunneling decay constant β was 0.90 per carbon (0.75 $Å^{-1}$) which is consistent with previously reported values using break junctions, scanning tunneling microscopy, electrochemistry, and large area devices.[2,8,17] The conductance peaks are nearly equally spaced with no clear trend in the spacing as the number of incorporated molecules increased. Peak broadening in the histograms is the summation of several effects: intrinsic broadening due to electromagnetic noise and thermal vibration at the molecule/Au interface, broadening due to various contact and molecular geometries, and the possibility of a change in the number of contacted molecules during the acquisition of a data point. The absolute value of our measured molecular conductance is within an order of magnitude of previously reported values for individual alkane molecules.[18] In contrast to most single molecule measurements, our molecules are incorporated in a monolayer with potential electronic and structural interactions between adjacent molecules. We expect that

Table 1. Molecular conductance of seven molecules from a total of 25 junctions[a]

molecule	no. of fabricated junctions	total no. histogram peaks	average ± stardard deviation peak spacing (G_o × 10^{-5})
C_4−NH	3	21	75 ± 15
C_6−NH	3	17	10.2 ± 1.9
C_8−NH	3	13	1.39 ± 0.23
C_{10}-NH	2	10	0.32 ± 0.07
NAB	5	27	2.0 ± 0.4
AB	4	22	20 ± 3
DAB	5	27	69 ± 11

[a] Spacing between histogram peaks stated in units of G_o × 10^{-5}, e.g. C_4 has a conductance of 75 × 10^{-5} G_o, or 58 nS. Histograms showing a total of 137 conductance peaks were constructed from the 25 current-time traces, and centers of the conductance peaks were determined from Lorentzian fits.

comparison between in situ SDMD and break junction techniques will provide critical insights into the role of contact chemistry and intermolecular effects.

To investigate the effect of molecular energy levels on charge transport, conductance through a series of azobenzene (AB) monolayers with similar lengths but varying orbital energies was measured, with the results listed in Table 1. For nitroazobenzene (NAB), the electron withdrawing nitro group lowers the highest

dx.doi.org/10.1021/nl202495k |*Nano Lett.* 2011, 11, 4725–4729

Table 2. Measured and Calculated Electronic Properties for Three Azobenzene Molecules[a]

molecule (length, Å)	G_{mol} (G_o x 10^{-5})	dipole (D)	HOMO (eV)	LUMO (eV)	E_F^{mol} (eV)
NAB (12.8)	2.0 ± 0.4	7.2	−6.7	−3.0	−5.1
AB (11.7)	20 ± 3	0.0	−6.1	−2.2	−4.8
DAB (14.0)	69 ± 11	−4.6	−5.0	−1.5	−4.5

[a] The molecular conductance (G_{mol}) was determined from the average peak spacing of five histograms for five NAB junctions, four AB, and five DAB junctions (see Supporting Information for detailed statistics). Molecular lengths, dipoles, and energy levels calculated with Gaussian '03 using DFT B3LYP/6-31G(d). Stated energies and Fermi levels are relative to vacuum. E_F^{mol} was determined with ultraviolet photoelectron spectroscopy.

occupied molecular orbital (HOMO) energy and decreases the single molecule conductance by a factor of 10 compared to AB. The electron donating dimethylamino group in dimethylaminoazobenzene (DAB) raises the HOMO energy and results in a 5-fold increase of conductance compared to AB, despite the longer tunneling distance for DAB. This trend of higher conductance when the HOMO energy is closer to the bulk Fermi level (E_F^{bulk} = −4.9 eV) of the carbon sidewall provides strong evidence for HOMO transport through azobenzene molecules and shows that conductance modification through end group tailoring can be achieved, thus providing a critical step toward rational design.

For off-resonant tunneling through molecules, it is commonly accepted that molecular conductance (G_{mol}) can be modeled as

$$G_{mol} \propto Ae^{(-d\sqrt{\phi})}$$

where A is a constant, d is the molecule length, and ϕ is the tunneling barrier. For HOMO tunneling, the tunneling barrier can be approximated by the difference between the molecular HOMO and the Fermi energy (E_F) of the contact electrode. Included in Table 2 are the calculated HOMO energies of the free molecules and the interfacial work function (E_F^{mol}) of the carbon contact with its respective bonded monolayer, as determined by ultraviolet photoelectron spectroscopy.[19] The change measured in the E_F^{mol} relative to the bulk E_F is consistent with the associated molecular dipole of the monolayer.[20] Plots of the natural logarithm of the observed molecular conductance versus $d\sqrt{\phi}$ are shown in Figure 4a, with the barrier determined either as $E_F^{bulk} - E_{HOMO}$ or $E_F^{mol} - E_{HOMO}$. The slopes in Figure 4a differ due to the effect of the molecular dipole on the apparent E_F of the carbon contact, but in both cases there is a monotonic dependence which is consistent with off-resonant tunneling through the HOMO. The effect of the molecular dipole on the HOMO and interfacial E_F energies are in the same direction, resulting in a smaller conductance change than expected through consideration of the HOMO energy change alone. Although there are too few points to confirm linearity, it is interesting to note that extrapolation of the least-squares line for the $E_F^{mol} - E_{HOMO}$ data to $d\sqrt{\phi} = 0$ yields an intercept of 0.95 G_o. It is very reasonable to expect the conductance to approach that of a direct Au−C contact when the barrier height or tunneling distance approach zero. The molecular conductance does not correlate with the LUMO energies, supporting the conclusion that HOMO tunneling is the operative transport mechanism (see Supporting Information). A similar mechanism has been proposed for tunneling through the HOMOs of single molecules,[21] although the range of observed conductance values was significantly smaller. Since the SDMD technique does not require chemisorption at the molecule/Au interface, the conductance of para-substituted azobenzene molecules could be measured. With the Au contact

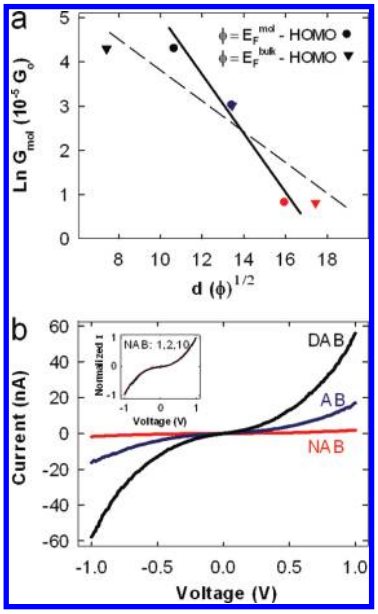

Figure 4. Electronic characteristics of a series of azobenzene molecules. (a) Plot of the natural logarithm of the measured molecular conductance verss $d\sqrt{\phi}$ for three azobenzene molecules, where d is the calculated molecular length and ϕ is estimated from the difference between the calculated HOMO energy and either the bulk E_F or interfacial E_F^{mol} of the carbon sidewall. (b) $I-V$ curves of junctions containing single NAB, AB, or DAB molecules, as determined by counting the observed conductance steps. Inset shows the normalized $I-V$ curves for 1, 2, and 10 NAB molecules showing minimal change in curvature as the number if incorporated conducting molecules increases.

only physisorbed to the molecules, minimal charge transfer is expected to result in only a weak effect of the molecule/Au interaction on the molecular conductance, although a stronger effect is expected for a chemisorbed contact. Since the conduction is governed by tunneling, the conductance modulation is most likely caused by the effect of para-substitution on the HOMO energies. These results show the importance of the molecular dipole as well as the energetics of the entire system on the molecular conductance.

In situ SDMD allows acquisition of current−voltage ($I-V$) curves at any point during deposition, where the number of incorporated molecules is determined by counting the preceding conductance steps. Figure 4b shows $I-V$ curves for molecular junctions containing single NAB, AB, or DAB molecules, and fitting the curves with an off-resonance model results in tunneling barriers $\phi_{DAB} < \phi_{AB} < \phi_{NAB}$, consistent with the previous conclusions and calculations from large-area junctions (Supporting Information). Note that tunneling is nondissipative, and should not cause local heating of the molecules even at the high current

dx.doi.org/10.1021/nl202495k |Nano Lett. 2011, 11, 4725–4729

densities represented by ~10 nA through a single molecule. The $I-V$ curves showed no changes with scan rate or maximum current, as might be expected for local heating. The symmetry of the $I-V$ curves of Figure 4 is consistent with off-resonant tunneling, which depends strongly on the tunneling distance and average barrier height, but weakly on the difference in the work functions of the contacts. Symmetric $I-V$ curves from compositionally asymmetric molecular junctions have been reported in the literature, such as Ag−S−molecule/eGaIn,[22] Au−S−molecule/Au,[23] Au−dithiol/PEDOT−PSS[3], and Au−S−alkane−COOH/Al_2O_3/Au[24] junctions. Since conduction through our junctions does not involve charge injection and the contact work functions differ by only 0.15 eV,[13] nearly symmetric $I-V$ curves are expected. In addition, we previously showed that a change in the work function of the top contact by greater than 1 eV changed the symmetry of similar molecular junctions by only a factor of 3.[8] The inset in Figure 4b shows overlaid $I-V$ curves for junctions containing 1, 2, and 10 NAB molecules normalized to the same maximum current, showing that the curvature is invariant as the junction conductance increased. This result is consistent with equal conductance peak spacing in the histograms and indicates either that conductance is additive for the increasing number of conducting molecules, or the contacted molecules are widely spaced on the molecular monolayer. Although possible, sequentially contacting 6−10 widely spaced molecules within a monolayer by the diffusing Au contact is unlikely. This trend was observed for all aliphatic and aromatic molecules studied, suggesting that molecular conductance within a molecular layer is additive with the number of conducting molecules, at least for junctions containing less than ten molecules in parallel. It should be noted, however, that the conductance "per molecule" reported for "large area" junctions of the same molecules[4,8,25] is significantly lower than the single-molecule conductance reported herein, implying that additivity does not apply when a large number of molecules are oriented in parallel. We are currently investigating the reasons for this discrepancy, by extending the series of $I-V$ curves shown in Figure 4b (inset) to much larger junction areas.

The in situ SDMD paradigm is amendable to a variety of materials, as well as a wide range of molecular structures with different energy levels, dipoles, and conjugation. The ability to monitor conductance in situ during contact formation with single-molecule resolution suggests additional applications, such as conductance measurements on biological molecules, fullerenes, and conjugated polymers.

■ ASSOCIATED CONTENT

Supporting Information. Additional information and figures. This material is available free of charge via the Internet at http://pubs.acs.org.

■ AUTHOR INFORMATION

Corresponding Author

*Tel.: 780-641-1760. E-mail: richard.mccreery@ualberta.ca.

■ ACKNOWLEDGMENT

This work was supported by the National Science Foundation, Alberta Innovates Technology Futures, and The National Institute for Nanotechnology, and the National Research Council of Canada. The authors would like to acknowledge Dr. Ken Harris and Dr. Haijun Yan for scientific discussions and Bryan Szeto for technical support. A.P.B performed the experiments and A.P.B and R.L.M conceived and designed the experiments, analyzed the data, and wrote the main and supplementary manuscripts. The authors declare no competing financial interests.

■ REFERENCES

(1) (a) Park, J.; Pasupathy, A. N.; Goldsmith, J. I.; Chang, C.; Yaish, Y.; Petta, J. R.; Rinkoski, M.; Sethna, J. P.; Abruna, H. D.; McEuen, P. L.; Ralph, D. C. *Nature* **2002**, *417*, 722–725. (b) Reed, M. A.; Zhou, C.; Muller, C. J.; Burgin, T. P.; Tour, J. M. *Science* **1997**, *278*, 252–254.

(2) Xu, B. Q.; Tao, N. J. J. *Science* **2003**, *301*, 1221–1223.

(3) Akkerman, H. B.; Naber, R. C. G.; Jongbloed, B.; van Hal, P. A.; Blom, P. W. M.; de Leeuw, D. M.; de Boer, B. *Proc. Natl. Acad. Sci. U.S.A.* **2007**, *104*, 11161–11166.

(4) Ru, J.; Szeto, B.; Bonifas, A.; McCreery, R. L. *ACS Appl. Mater. Interfaces* **2010**, *2*, 3693–3701.

(5) McCreery, R. L.; Bergren, A. J. *Adv. Mater.* **2009**, *21*, 4303–4322.

(6) (a) Blum, A. S.; Kushmerick, J. G.; Long, D. P.; Patterson, C. H.; Yang, J. C.; Henderson, J. C.; Yao, Y. X.; Tour, J. M.; Shashidhar, R.; Ratna, B. R. *Nat. Mater.* **2005**, *4*, 167–172. (b) Donhauser, Z. J.; Mantooth, B. A.; Kelly, K. F.; Bumm, L. A.; Monnell, J. D.; Stapleton, J. J.; Price, D. W.; Rawlett, A. M.; Allara, D. L.; Tour, J. M.; Weiss, P. S. *Science* **2001**, *292*, 2303–2307.

(7) (a) Osorio, E. A.; O'Neill, K.; Wegewijs, M.; Stuhr-Hansen, N.; Paaske, J.; Bjornholm, T.; van der Zant, H. S. J. *Nano Lett.* **2007**, *7*, 3336–3342. (b) Song, H.; Kim, Y.; Jang, Y. H.; Jeong, H.; Reed, M. A.; Lee, T. *Nature* **2009**, *462*, 1039–1043.

(8) Bonifas, A. P.; McCreery, R. L. *Nat. Nanotechnol.* **2010**, *5*, 612–617.

(9) Ibach, H. *Physics of Surfaces and Interfaces*, 1st ed.; Springer: New York, 2006.

(10) Ittah, N.; Yutsis, I.; Selzer, Y. *Nano Lett.* **2008**, *8*, 3922–3927.

(11) (a) Bhattacharyya, S.; Henley, S. J.; Mendoza, E.; Gomez-Rojas, L.; Allam, J.; Silva, S. R. P. *Nat. Mater.* **2006**, *5*, 19–22. (b) Asaka, K.; Kato, R.; Yoshizaki, R.; Miyazawa, K.; Kizuka, T. *Phys. Rev. B* **2007**, *76*, 3.

(12) Agrait, N.; Yeyati, A. L.; van Ruitenbeek, J. M. *Phys. Rep.* **2003**, *377*, 81–279.

(13) Yan, H. J.; McCreery, R. L. *ACS Appl. Mater. Inter.* **2009**, *1*, 443–451.

(14) Anariba, F.; DuVall, S. H.; McCreery, R. L. *Anal. Chem.* **2003**, *75*, 3837–3844.

(15) Anariba, F.; Viswanathan, U.; Bocian, D. F.; McCreery, R. L. *Anal. Chem.* **2006**, *78*, 3104–3112.

(16) Mujica, V.; Ratner, M. A. *Chem. Phys.* **2001**, *264*, 365–370.

(17) (a) Akkerman, H. B.; Blom, P. W. M.; de Leeuw, D. M.; de Boer, B. *Nature* **2006**, *441*, 69–72. (b) Engelkes, V. B.; Beebe, J. M.; Frisbie, C. D. *J. Am. Chem. Soc.* **2004**, *126*, 14287–14296. (c) Liu, B.; Bard, A. J.; Mirkin, M. V.; Creager, S. E. *J. Am. Chem. Soc.* **2004**, *126*, 1485–1492.

(18) (a) Li, C.; Pobelov, I.; Wandlowski, T.; Bagrets, A.; Arnold, A.; Evers, F. *J. Am. Chem. Soc.* **2008**, *130*, 318–326. (b) Venkataraman, L.; Klare, J. E.; Tam, I. W.; Nuckolls, C.; Hybertsen, M. S.; Steigerwald, M. L. *Nano Lett.* **2006**, *6*, 458–462.

(19) (a) Hunger, R.; Jaegermann, W.; Merson, A.; Shapira, Y.; Pettenkofer, C.; Parrich, J. *J.Phys. Chem. B* **2006**, *110*, 15432. (b) Colavita, P. E.; Sun, B.; Wang, X. Y.; Hamers, R. J. *J. Phys. Chem. C* **2009**, *113*, 1526.

(20) Vilan, A.; Shanzer, A.; Cahen, D. *Nature* **2000**, *404*, 166–168.

(21) Venkataraman, L.; Park, Y. S.; Whalley, A. C.; Nuckolls, C.; Hybertsen, M. S.; Steigerwald, M. L. *Nano Lett.* **2007**, *7*, 502–506.

(22) Nijhuis, C. A.; Reus, W. F.; Whitesides, G. M. *J. Am. Chem. Soc.* **2009**, *131*, 17814–17827.

(23) Choi, S. H.; Kim, B.; Frisbie, C. D. *Science* **2008**, *320*, 1482–1486.

(24) Preiner, M. J.; Melosh, N. A. *Appl. Phys. Lett.* **2008**, *92*, 213301–213303.

(25) Bergren, A. J.; McCreery, R. L.; Stoyanov, S. R.; Gusarov, S.; Kovalenko, A. *J. Phys. Chem. C* **2010**, *114*, 15806–15815.